Supplementary Information for:

Impact of Nitrogen, Boron and Phosphorus Impurities on the Electronic Structure of Diamond Probed by X-ray Spectroscopies

Sneha Choudhury[1,2], Ronny Golnak[1], Christian Schulz[1], Klaus Lieutenant[1], Nicolas Tranchant[3], Jean-Charles Arnault[3,+], Marie-Amandine Pinault-Thaury[4], François Jomard[4], Peter Knittel[5], Tristan Petit[1,*]

[1] *Helmholtz-Zentrum Berlin für Materialen und Energie GmbH, Albert-Einstein-Str. 15, 12489 Berlin, Germany*

[2] *Department of Chemistry, Freie Universität Berlin, Arnimallee 14, 14195 Berlin, Germany*

[3] *CEA, LIST, Diamond Sensors Laboratory, 91191 Gif-sur-Yvette, France*

[4] *Université Paris-Saclay, UVSQ, CNRS, GEMaC, 78000 Versailles, France*

[5] *Fraunhofer Institute for Applied Solid State Physics, Tullastraße 72, 79108 Freiburg, Germany*

[*] *tristan.petit@helmholtz-berlin.de*

[+] *Current address : NIMBE, UMR CEA-CNRS 3685, Université Paris-Saclay, 91191 Gif-sur-Yvette, France*

1 Differential interference contrast microscopy

Differential interference contrast (DIC) microscopy has been performed on doped samples at GEMaC with a Nikon ECLIPSE ME600L microscope. The surfaces of the three samples are shown in Figure S1. B-SCD presents a smooth surface while the surface of P-SCD sample is rough with some straight marks. The N-SCD surface is partly covered of typical hillocks with unepitaxial crystallites on top of them. B-SCD and P-SCD have been imaged before SIMS analysis, unlike N-SCD sample. For this reason, SIMS craters (squares) resulting of the N content analysis are visible on the N-SCD surface. For all samples, the spectroscopic analysis has been performed in areas free of structural defects.

B-SCD (a) P-SCD (b) N-SCD (c)

Figure S1: Differential interference contract (DIC) microscopy of (a) B-SCD, (b) P-SCD, and (c) N-SCD samples.

2 Secondary Ion Mass Spectrometry analysis

Secondary Ion Mass Spectrometry (SIMS) has been performed in order to measure the depth distribution of the boron ([B]), phosphorus ([P]) and nitrogen ([N]) concentrations in B-SCD, P-SCD and N-SCD samples, respectively. Prior to SIMS analysis a gold film of ~50 nm is deposited to avoid any charging effect during measurements. A CAMECA IMS7f equipment was used. The vacuum limit reached in the analysis chamber was of $\sim 10^{-9}$ mbar. The depth of the resulting 150x150 µm² SIMS crater was measured using a Dektak8 step-meter. The analyzed zone is restricted to a diameter of 33 µm to limit the crater edge effects.

As the SIMS technique is mostly used in diamond to detect impurities, measurements are performed by using parameters allowing high sensitivities for studied elements. Namely, the Cs^+/M^- configuration is classically employed (positive primary ions with a Cs^+ source and detection of negative secondary ions of mass M). The energy of the Cs^+ primary beam is set to 10 keV. Secondary ions are detected in the negative mode (the sample is biased to −5000 V) leading to an interaction energy of the primary ions of 15 keV and an incidence angle of 23° with respect to the normal of the sample. In this study, the current of the Cs^+ ion beam is set at 40 nA allowing a sputtering rate of ~ 0.3 nm/s.

Analysis of boron and phosphorus was performed by detecting secondary ions of masses 12 (carbon), 11 (boron), 31 (phosphorus). These routine analyses have been done at a low mass resolution, $M/\Delta M = 400$, to have a maximum sensitivity. On the contrary, analysis of nitrogen by SIMS presents a specific issue as the secondary ion yield for N^- is essentially zero. Then, nitrogen is usually analyzed by means of a molecular species. For diamond samples, the molecular ion CN^- has high intensity. However, detecting secondary ion of mass 26 in diamond presents another issue. At such mass value, several molecular species can be detected in diamond in addition to $^{12}C^{14}N$ (26.0031 u.): $^{13}C_2$ (26.0067) and $^{13}C^{12}C^{1}H$ (26.0112). It is possible to separate them by working at high mass resolution, HMR ($M/\Delta M \sim 6000$), at the expense of sensitivity. In our study, the reduction factor is ~15 for the matrix signal (^{12}C) that is the most intense signal.

Figure S2 shows the mass spectra of 3 samples analyzed in the HMR of $M/\Delta M \sim 6000$: a type Ib HPHT diamond substrate (known to contain high nitrogen level, in the range of a few 10^{19} at/cm^3), a non-intentionally nitrogen doped SCD (where very low nitrogen level is expected, named NID sample) and an intentionally nitrogen doped SCD (obtained by adding nitrogen during its CVD growth). In such HMR conditions the mass spectra exhibit 3 separated peaks. In the middle, the $^{13}C_2$ peak (that is characteristic of the diamond matrix) is used to normalized the spectra to its intensity.

On the left, at higher mass, the $^{13}C^{12}C^{1}H$ peak is observed for all samples at different intensities due to residual hydrogen in the analysis chamber and around the analysis area. On the right, at lower mass, the $^{12}C^{14}N$ peak reveals, as expected, the presence of nitrogen in the intentionally nitrogen doped SCD with an intensity in between the one of the NID sample, which has the lowest intensity, and the one of the HPHT Ib substrate, which presents the highest intensity.

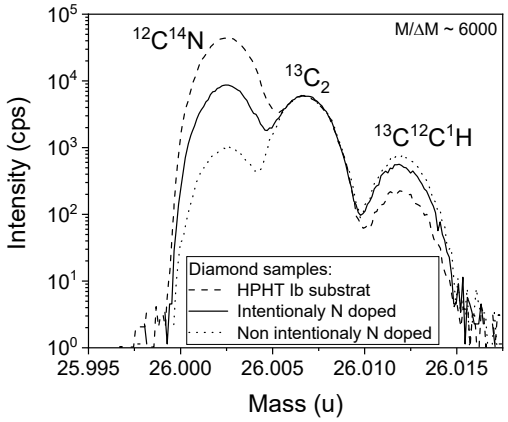

Figure S2: Mass spectra around the 26 mass in high mass resolution (HMR) of M/ΔM ~ 6000 for 3 different diamond samples: a type Ib HPHT substrate (that contain a high level of nitrogen), a non-intentionally nitrogen doped SCD (containing a very low nitrogen level) and an intentionally nitrogen doped SCD (obtained by adding nitrogen during its CVD growth).

To quantify the ^{11}B, ^{31}P and $^{14}N^{12}C$ intensities, implanted standards with a known dose of each isotope are also analyzed by SIMS in the same conditions than their counterpart SCD samples. The profiles of the implanted standards allow to extract the relative sensitivity factor (RSF) of each studied element. The RSF values are then implemented together with the depth of the crater to quantify data. The following RSF values have been obtained: $4.7x10^{24}$ at/cm^3 for $^{11}B/^{12}C$, $1.8x10^{23}$ at/cm^3 for $^{31}P/^{12}C$, and $2.2x10^{22}$ at/cm^3 for $^{14}N^{12}C/^{12}C$. The analysis of the implanted standard profiles gives also access to the detection limit of the analyzed element. In our study, the values of the detection limits are: $1.5x10^{15}$ at/cm^3 for boron, $3.3x10^{14}$ at/cm^3 for phosphorus, and $1.2x10^{17}$ at/cm^3 for nitrogen (as an atmospheric element, this high value is due to the residual vacuum of the equipment).

Figure S3 shows the depth profiles of the 3 samples over the first 300 nm probed from their surfaces. In our study, the SIMS analysis conditions induce a pre-equilibrium region of ~25 nm from which no clear quantitative information can be extracted from the profiles. This region is symbolized by a dashed rectangle on figure 2. For the B-SCD and N-SCD samples, the impurity concentrations are constant with plateaus of [B] ~ $2.7x10^{20}$ at/cm^3 and [N] ~ $4.9x10^{18}$ at/cm^3, respectively. The

phosphorus content of P-SCD sample presents a weak increase in the first 150 nm by a factor ~ 1.5 in the content up to a plateau of [P] ~$8.0x10^{19}$ at/cm^3.

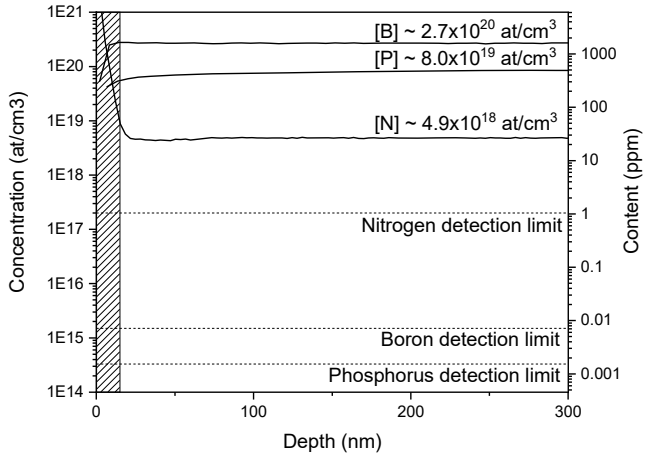

Figure S3: SIMS depth profiles of boron for the B-SCD sample, of phosphorus for the P-SCD sample and of nitrogen for the N-SCD sample. The concentration values are averaged over the probed depth. The dashed lines are the detection limits. The dashed rectangle represents the pre-equilibrium region of the SIMS profile from which no clear quantitative information can be extracted (this region depends on the SIMS analysis conditions).

The SIMS analysis give then access to the impurity content in each sample in the depth probed by the spectroscopic measurements (the first 150 nm from the surface): [B] ~ 1500 ppm, [P] ~ 400 ppm and [N] ~ 30 ppm respectively for B-SCD, P-SCD and N-SCD samples.

3 Resonant Photoemission Spectroscopy at the C K-edge

The XPS C1s of the different diamond samples was acquired at an excitation energy of 500 eV to ensure a high surface sensitivity (Figure S4). As mentioned in the main manuscript, photoelectrons could not be detected from the N-SCD. For P-SCD, the C1s peaks appears significantly broadened and shifted of 6.15 eV toward higher energy. This energy shift was found to depend on the excitation energy and is therefore most likely not related to a chemical shift but rather to charging effects.

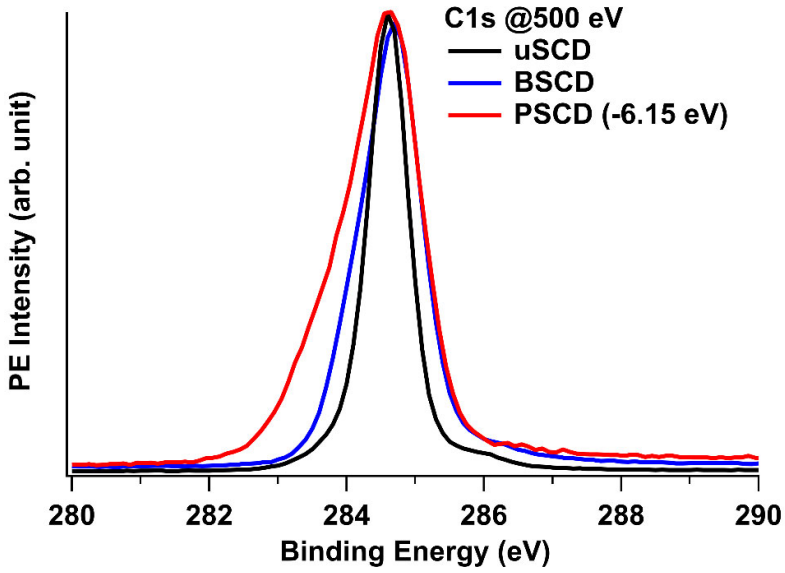

Figure S4: XPS C1s spectra of uSCD, BSCD and PSCD measured with a 500 eV excitation energy. The charging effect on PSCD sample was corrected by shifting the spectrum by -6.15 eV.

The valence band of the different diamond samples was further characterized by resonant photoemission spectroscopy (RPES), which means that the excitation energy is tuned to excite resonantly different features visible on the XAS. As visible on Figure S5, C1s photoelectrons (excited by second order light) are overlapping with the valence electrons. Knowing that the C1s peak maximum is situated at 284.6 eV, the second order C1s peak can be used to correct the charging effect by shifting the RPES spectra until the C1s peak reaches the expected (kinetic) energy. For easier comparison of the spectra, they are plotted with respect to binding energy related to the valence band levels.

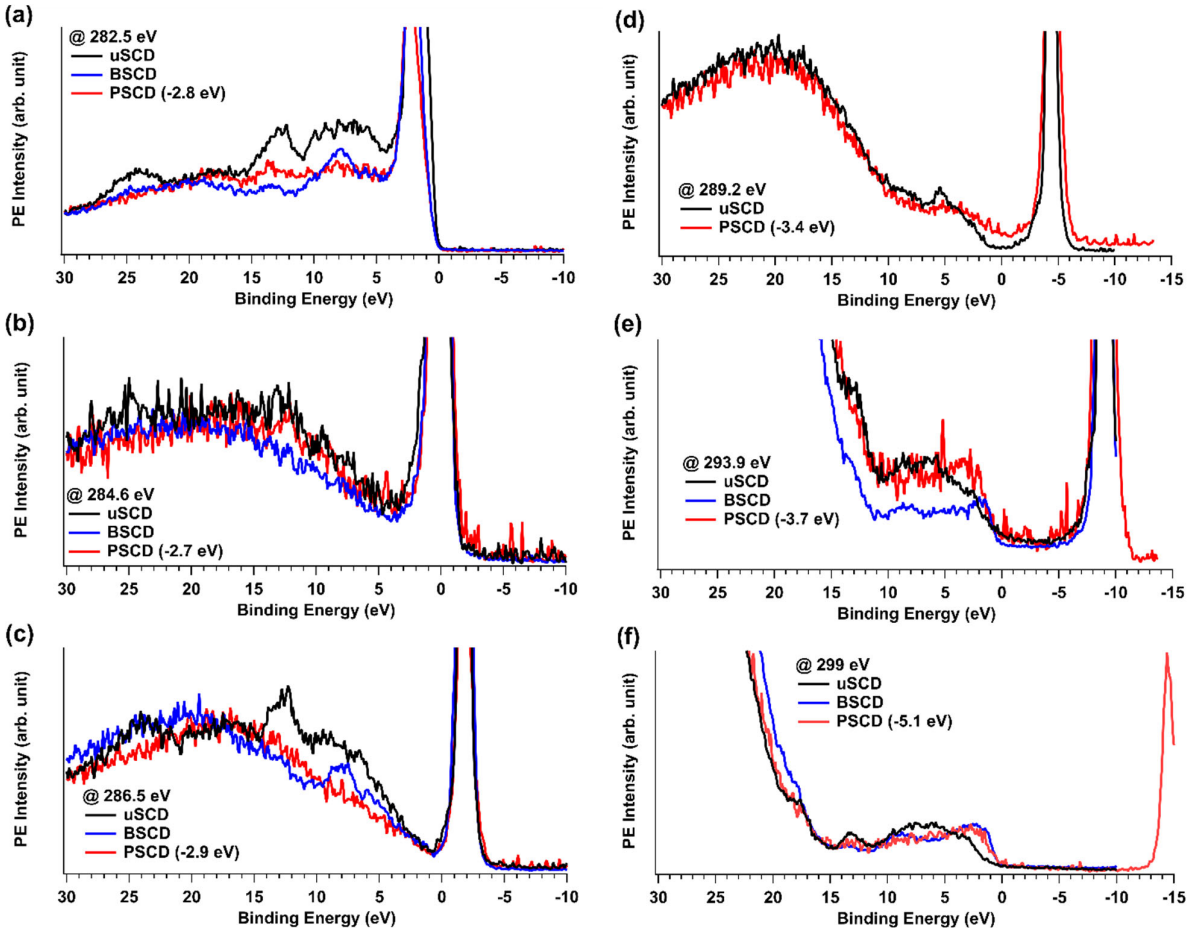

Figure S5: Resonant photoemission spectra of the valence band range of uSCD, B-SCD and P-SCD at 282.5 (a), 284.6 (b), 286.5 (c), 289.2 (d), 293.9 (e) and 299 eV (f) excitation energies. The spectra are plotted with respect to binding energy related to the valence band region. The charging effect on P-SCD sample was corrected by shifting the spectrum of the value indicated in the legend. The spectra were normalized to the signal in the region around 20-30 eV.

Upon resonant excitation below 286.5 eV, the feature around 12 eV is enhanced for uSCD while the peak around 8 eV appears particularly clear for B-SCD. For energy above 289.2 eV, an intense broad band with binding energy >10 eV is appearing, shifting with the excitation energy, which is related to Auger electrons as the excitation energy is above the photoionization threshold of the C K-edge. A detailed understanding of these resonant features would require theoretical modelling, which is beyond the scope of this study.